Research Article BEU Fen Bilimleri Dergisi 15(2): 793-812 (2026) DOI: 10.17798/bitlisfen.1835627

BİTLİS EREN UNIVERSITY
FEN BİLİMLERİ DERGİSİ
ISSN: 2147-3129 / e-ISSN: 2147-3188

NONLINEAR DYNAMIC ANALYSIS AND RETROFITTING DESIGN OF AN EARTHQUAKE DAMAGED MASONRY BUILDING

Alper ÖZMEN [1*], Talha SARICI [1]

[1] *Inonu University, Civil Engineering Department, Malatya, Türkiye*
**** Corresponding Author:*** *alper.ozmen@inonu.edu.tr*

Article Info

Received: *December 3, 2025*
Revised: *April 20, 2026*
Accepted: *April 20, 2026*

Keywords
Residential Masonry,
Failure Mechanism,
Masonry Retrofitting,
2023 Kahramanmaraş Earthquakes,
Steel Stirrup.

ABSTRACT

Masonry buildings constitute a significant portion of the building stock in settlements situated along the East Anatolian Fault. Seismic risk is quite high in this region. This study investigates the earthquake response and retrofitting design of a residential masonry that damaged in the 2023 Kahramanmaraş earthquakes. Within the scope of the study, the existing damage condition and material properties of the structure were first determined. Using the collected data, the current state of the structure was analyzed with nonlinear dynamic analyses. Subsequently, potential damage zones were retrofitted using an innovative reinforcement method taken from the literature, and the results were compared. The retrofitting intervention reduced maximum displacement demand by approximately 33.3%, crack width by 26.5%, and inter-story drift ratio by nearly 54.8%. By combining field damage observations with nonlinear time-history analyses and implementing a validated steel-stirrup strengthening scheme, this study provides a practical and transferable methodology for improving the seismic performance of earthquake-damaged masonry buildings in high-risk regions.

1. INTRODUCTION

Masonry buildings constitute a substantial portion of the residential building stock in many developing regions because of their low construction cost and favorable thermal performance. However, unreinforced masonry structures generally exhibit limited tensile strength, low ductility, and poor energy dissipation capacity, which make them highly vulnerable to earthquake-induced damage [1]. For this reason, assessing the seismic response of existing masonry buildings and identifying effective strengthening strategies remain important research topics. Retrofitting approaches for masonry structures generally aim either to reduce seismic demand or to improve the lateral load-carrying capacity, stiffness, and deformation capacity of structural members [2–4].

On February 6, 2023, two major earthquakes with magnitudes of Mw 7.6 and 7.7, respectively, affected the eastern cities of Türkiye. The earthquakes affected a wide region in southern and eastern Türkiye, including Kahramanmaraş, Hatay, Adıyaman, Gaziantep, Malatya, Kilis, Diyarbakır, Adana, Osmaniye, Şanlıurfa, and Elazığ, which collectively house around 15 million individuals. Studies indicate that these seismic events resulted in 50,783 fatalities in Türkiye and 8,476 in Syria [5]. Moreover, the earthquakes destroyed or severely compromised 214,577 structures. Malatya is one of the cities most affected by these earthquakes [6]. Many buildings in the city center and districts of Malatya have collapsed and suffered severe damage. Malatya province also has a lot of masonry structures. Following the 2023 Kahramanmaraş earthquakes, many of these masonry buildings have also suffered significant damage or have collapsed (Figure 1). Therefore, it is vital to evaluate the seismic performance of masonry structures. There are numerous numerical studies in the literature that examine the seismic performance of masonry constructions. Uzdil et al. [7] provides a seismic performance evaluation of a historically significant masonry building originally demolished in the 1940s, with a focus on its reconstruction. The research offers a detailed analysis of the structural vulnerabilities and proposes specific strengthening interventions to enhance the building's resilience against seismic events. Damiani et al. [8] examine a numerical evaluation of a timber retrofit method intended to raise the unreinforced masonry buildings'

License: CC BY-NC 4.0

seismic performance. The study provides an affordable and efficient means of seismic retrofitting old masonry structures by showcasing the effectiveness of timber retrofitting in boosting structural integrity and resilience through sophisticated modelling methodologies. Ranjbaran and Kianibakhsh [9] specifically examine the seismic performance of constrained masonry buildings, which are commonly found in areas prone to earthquakes, with a particular focus on displacement-based assessment. The research quantifies the displacements of buildings under simulated seismic loads. This gives valuable information about the behavior and vulnerabilities of restricted masonry structures. It also helps in developing better designs and retrofit strategies to handle displacement demands during earthquakes. Coşgun et al. [10] conduct an extensive evaluation of the seismic susceptibility of a current brick restaurant facility by utilizing a wide range of structural analyses to determine its performance during seismic events. The authors employed linear, nonlinear, and kinematic limit analysis techniques to determine the building's reaction to seismic forces, pinpointing critical vulnerabilities in its structural soundness. The study suggests a retrofitting approach utilizing fiber-reinforced polymer (FRP) composites to improve the building's ability to withstand seismic activity. The effectiveness of the proposed retrofit was further examined through the utilization of both linear and nonlinear approaches, providing a compelling argument for its implementation in similar masonry structures that are vulnerable to seismic activity. Bilgin and Korini [11] were carried out to assess the seismic performance of three different masonry structures, with consideration given to nonlinear dynamics. The researchers employed finite element software to develop models of the structures and produced capacity curves along the x and y axes using pushover analysis. The results were subsequently evaluated in compliance with the FEMA 440 guidelines. Çarhoğlu and Korkmaz [12] investigated the behavior of a masonry structure under seismic forces using the finite element approach. The authors conducted a time history dynamic analysis using twenty distinct earthquake acceleration records. Findings from the analysis indicated that the most significant stresses occurred during the earthquake that produced the largest displacements. Researchers have developed diverse methodologies to evaluate the seismic performance of masonry structures, encompassing linear analyses, nonlinear time history analyses, pushover analyses, and kinematic analyses [14-22].



Figure 1. Damaged masonry buildings in Malatya Province After 2023 Kahramanmaraş earthquakes [13]

Numerical modelling is widely used to evaluate the seismic response of masonry buildings, identify critical damage zones, and assess the effectiveness of possible retrofitting interventions. Previous studies have examined a wide range of strengthening techniques, including steel grid systems, stainless-steel strips, tie rods, FRP-based solutions, and textile-reinforced mortars, and have demonstrated that such interventions can significantly improve the stiffness, strength, and deformation capacity of masonry walls [23–33]. However, further research is still needed to better understand the seismic behaviour of masonry buildings that were damaged during highly destructive earthquakes and remained standing after the event. In particular, the 2023 Kahramanmaraş earthquake sequence highlighted the need to investigate real damaged masonry buildings in the affected region and to evaluate suitable retrofit strategies using field observations together with nonlinear numerical analyses.

In this study, a two-storey masonry residential building located in Malatya and damaged during the 6 February 2023 Kahramanmaraş earthquake sequence was selected as the case study. First, field

observations were used to document the building geometry, structural layout, and observed damage pattern. Then, a three-dimensional finite element model was developed in DIANA FEA, and nonlinear pushover and nonlinear time-history analyses were performed to evaluate the seismic response of the existing structure. Based on the identified damage-prone regions, a strengthening technique adopted from the literature was selected and implemented in the numerical model. The effect of the retrofitting intervention on the seismic behaviour of the building was then assessed through repeated nonlinear analyses.

2. A BRIEF DESCRIPTION AND DAMAGE SURVEY OF FIELD STUDY

The structure is located in Battalgazi province, a town of Malatya, Türkiye. The structure has 2 stories and is constructed with hollow brick. The thickness of the outer walls is 35 cm, while that of the inner walls is 19 cm. According to the field survey, the building is supported by a continuous strip foundation. The coordinates of the structure are 38°23'40.1"N 38°19'54.9"E. The location of the structure, obtained from Google Maps, is presented in Figure 2, while Figure 3 provides a general view of the building. A detailed structural system survey was carried out and information such as the layout of the structural system, the cross-sectional dimensions of the elements, the change between floors, story height, and the layout of the partition walls was obtained, and the structural system survey plans of the building were prepared. A plan view of the structure was presented in Figure 4.



Figure 2. Location of the structure



Figure 3. Some views of the structure

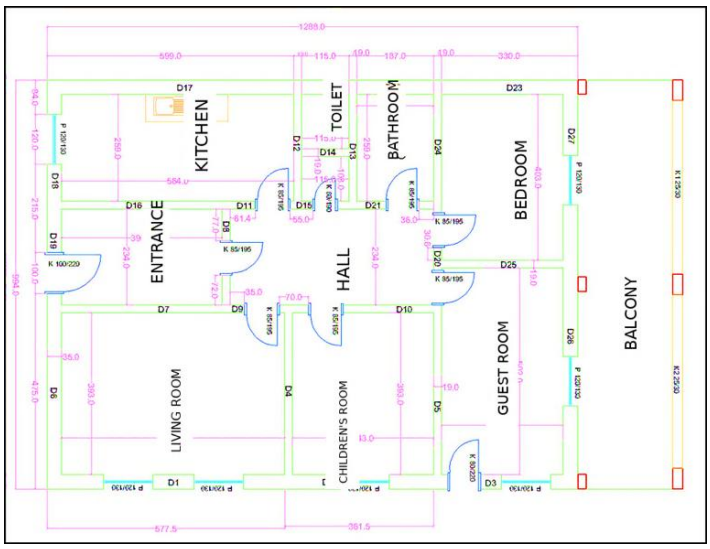


Figure 4. Plan view of the structure

2.1. Damage Survey of the Structure

After the 2023 Kahramanmaraş earthquakes, a post-earthquake damage survey of the structure was carried out. According to the visual inspection of the structure, no damage was observed on the exterior of the building. Structural cracks were observed at many different points on the interior walls (Figure 5). The cracking widths observed in the structure range from 1-2.5 mm. Observed damage in the investigated building was classified according to commonly reported earthquake-induced masonry damage patterns and established damage description frameworks. The dominant observed damage type was in-plane diagonal cracking in interior wall panels and around openings (Figure 5), accompanied locally by plaster spalling/delamination along crack paths. Measured crack widths ranged from 1.0 to 2.5 mm, which, when interpreted together with crack pattern and extent, indicate slight-to-moderate damage in the unreinforced masonry walls [34]. No exterior wall collapse and no clear out-of-plane wall failure were observed in the investigated building during the field survey. The dominant damage pattern was in-plane cracking concentrated in interior wall panels and around openings. Similar in-plane cracking patterns have been reported in regional post-earthquake studies on masonry buildings damaged during the 2023 Kahramanmaraş earthquake sequence; however, the present description refers specifically to the investigated building in Malatya [35-37]. The contribution of this study was to directly couple such field-based damage classification with nonlinear dynamic FE analyses and a validated retrofit configuration, enabling a mechanism-consistent evaluation of retrofit effectiveness for a real earthquake-damaged masonry building.



Figure 5. Some cracks in the structure

2.2. Soil Survey

The parameters of the soil on which the structure within the scope of this study was constructed were taken from the study carried out by Özcan [38] and Sarici and Özcan [39]. Accordingly, the relevant soil consists of the upper 50 cm of organic soil and coarse, gravelly, sandy, silty clay below it and has an alluvial formation (Qal). The drilling log created within the scope of the soil survey is given in Figure 6.

According to the available geotechnical data, the site consists of alluvial soil with medium to high plasticity and a groundwater level of approximately 4–6 m. The site was classified according to the relevant code provisions using Vs30 and SPT-based criteria, and no liquefaction potential was reported for the considered ground conditions [39-43]. These parameters were used only to characterize the site condition of the investigated building. As a result, it is possible to safely construct average-sized buildings on this soil profile once the organic layer has been removed from this soil environment and the foundation design is in accordance with the soil parameters. For high-rise or heavy structures, deep foundations and more detailed soil-structure interaction analysis should be considered. Although the building examined in this study should not have been damaged in the earthquake due to the low number of storeys, the organic soil layer was not excavated and replaced with granular fill and the foundation selection was not made in accordance with geotechnical parameters, which led to the occurrence of damages. Furthermore, as pointed out by Özcan [38], the characteristics of the foundation soil considered in this study are typical for the central districts of Malatya. In this respect, this study may be almost a reference for the central districts of Malatya.

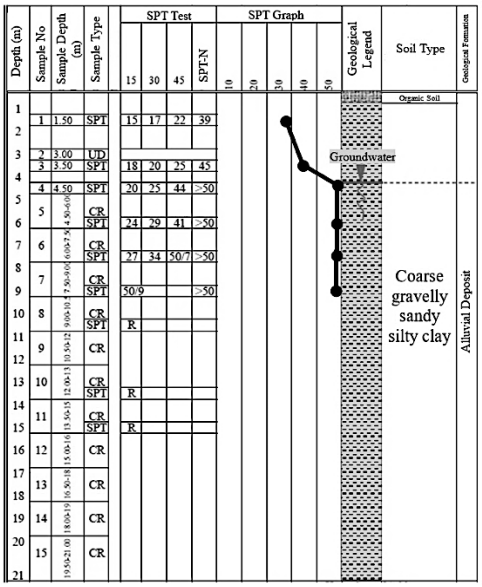


Figure 6. Drilling log

3. MATERIAL PROPERTIES OF THE STRUCTURE

Wall-unit samples were collected from the building to identify the masonry unit type and to verify the unit dimensions. Based on field observation and the collected samples, the walls were identified as being constructed with hollow clay brick units. Because a full laboratory characterization of the original units could not be performed within the scope of this study, the mechanical properties used in the numerical model were taken from the product catalogue of a comparable hollow clay brick unit [44]. The nominal dimensions of the hollow brick unit were 290 mm × 190 mm × 135 mm, corresponding to length × height × thickness, respectively. Therefore, the catalogue values were used as representative reference values rather than as exact certified properties of the original bricks in the investigated building (Table 1).

Table 1. Some properties of hollow brick

Properties	Weight (kg)	Unit weight (kg/m^3)	Thermal conductivity (W /mK)	Compressive strength (MPa)	Tensile Strength (MPa)	Poisson ratio
Value	4.7	1300	0.320	4	0.4	0.20

Utilizing the finite element method (FEM), three distinct modelling approaches have been devised for historic masonry structures, namely macro modelling techniques, simple micro modelling, and detailed micro modelling. This study utilized the macro modelling method, which treats masonry as a composite material, making no distinction between the bricks or stones and the mortar joints, as outlined by Lourenco [45]. Due to its reduced computational demands, the macro modelling approach is particularly suited for large-scale structural models [46-48]. Although the macro-modelling approach provides an efficient representation of the global structural behaviour, it cannot explicitly capture micro-level cracking, mortar joint separation, or local damage mechanisms occurring at the masonry unit level. Therefore, the obtained results should be interpreted primarily in terms of global structural performance. In order to obtain the linear elastic properties of the hollow brick, the main challenge is to determine the homogenized material properties of the masonry. Prior to this determination, two critical questions must be addressed: the properties of the mortar and the selection of the appropriate equation for calculating the homogenized material properties of the masonry [49-60]. In the macro-modelling approach, masonry is represented as a homogenized composite material rather than modelling brick units and mortar joints separately [45–48]. Therefore, representative material parameters had to be defined for the masonry assemblage. Because no direct experimental data were available for the mortar used in the investigated building, the mortar properties were adopted from representative values reported in the literature. A mortar compressive strength of 1 MPa and a Poisson's ratio of 0.05 were used in this study, which fall within the range commonly reported for weak mortars in similar masonry buildings [20, 50, 51]. These adopted values were then used together with relevant empirical relationships to define the homogenized properties of the masonry material used in the finite element model. In this study, the finite element model was developed using the macro modelling approach, wherein both mortar and masonry material are represented as a single material. Hence, some empirical formulas recommended by different researchers and standards were used for determining the composite material properties [52].

For the analyses in this study, DIANA FEA software was employed. The Total Strain-Based Crack Model (TSBCM) is the predominant material model used in the DIANA FEA software for simulating masonry structures. In this method, cracking is treated as a distributed effect along a single direction, and the material exhibiting cracks is modelled as a continuous medium possessing anisotropic properties, as stated in source DIANA FEA [61]. The Total Strain-Based Crack Model (TSBCM) utilized in DIANA FEA software delineates the behavior of materials under both tensile and compressive stresses through a unified stress-strain relationship. Within TSBCM, there are various methods to conceptualize behavior under tension and compression, including elastic, constant, and parabolic models. For the purposes of this study, the parabolic model will be employed, as depicted in Figure 7 [62]. The parameters essential for implementing the Total Strain-Based Crack Model include: density (ρ), elastic modulus (E), Poisson's ratio (ν), compressive strength (f_c), compressive fracture energy (G_c), tensile strength (f_t), and mode-1 fracture energy (G_f). Linear and nonlinear material homogenized material properties of case study structure was presented in Table 2.

The values reported in Table 2 represent homogenized masonry material parameters used in the finite element model, not directly measured properties of the individual brick units or mortar. These parameters were derived within the macro-modelling framework by combining the adopted brick-unit and mortar properties with empirical homogenization relationships reported in the literature. Therefore, the values of E, f_c, f_t, ν, G_c, and G_f given in Table 2 correspond to the equivalent masonry assemblage used in the nonlinear numerical analyses.

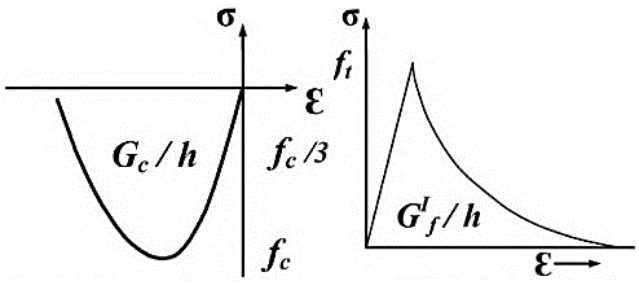


Figure 7. Behaviour of the Total Strain Based Crack Model under compressive (left) and tensile typical conditions (right) [61]

Table 2. Homogenized material properties of FEM

Property	Value
E (MPa)	1850
***Fc* (MPa)**	1.85
***Ft* (MPa)**	0.19
$\gamma_{masonry}$ **(g/cm^3)**	2.04
v	0.16
Gc	4.85
Gf	0,0125

4. NUMERICAL MODELLING OF STRUCTURE

A finite element model (FEM) was created using DIANA FEA finite element software [61]. In the finite element analysis of the structure, the TE12L element was employed. This element, characterized by its solid tetrahedral geometry with four nodes and three faces, is capable of exhibiting cracking behavior under tensile stress and crushing under compressive stresses. The finite element model included the masonry walls, slabs, and roof components of the building. The foundation system was not included explicitly in the numerical model. Since the slabs and roof were reinforced concrete members, they were modelled as concrete components; however, the reinforcing bars were not represented separately, and no damage evaluation was considered for these elements in the present study.

The finite element model consists of 34095 solid TE12L element and 11073 nodes. A mesh sensitivity analysis was carried out to determine the optimum mesh size suitable for masonry elements. The mesh size of 50 cm adopted for the masonry elements was selected based on the results of the mesh sensitivity analysis performed during the modelling stage. An automatic mesh generation procedure was used to create the finite element discretization of the structure. The FEM model of the structure was given in Figure 8. The control points used in the pushover and nonlinear time-history analyses were located at the upper level of the structure, near the roof elevation, in positions representative of the global lateral displacement response in the principal analysis directions.

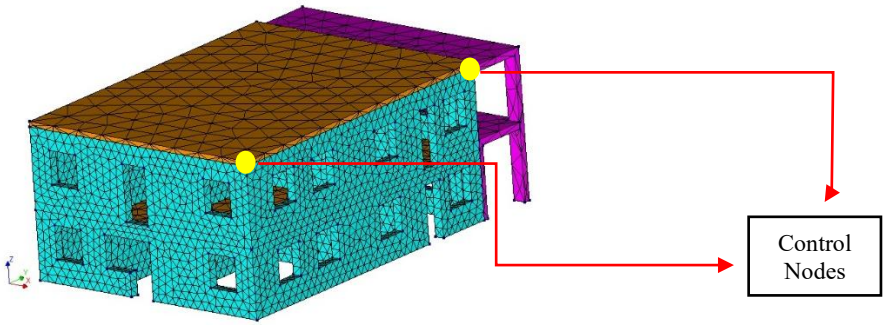


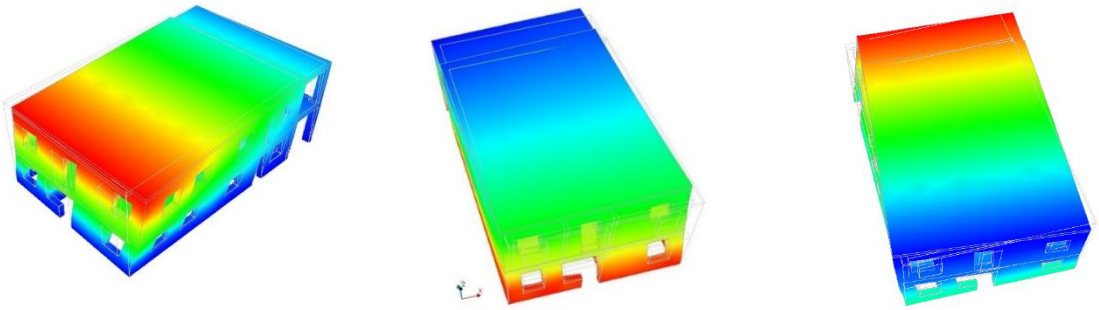
Figure 8. The FEM model of the structure

5. RESULTS FOR THE CURRENT STATE OF THE STRUCTURE

In this part of the study, modal analyses, non-linear static analyses, and non-linear dynamic analyses have been carried out and the results have been presented. Analyses were carried out on the current state of the structure before it was retrofitted.

5.1. Modal Analyses

A modal (eigenfrequency) analysis was conducted using a three-dimensional finite element model (FEM) to preliminarily evaluate the dynamic behavior of the structure. This analysis reveals the deformed configurations associated with effective vibration modes, which are defined by their mass participation ratios (MPR) and the corresponding periods [63, 64]. The first 3 mode shapes and vibration frequencies of finite element model of the structure are displayed in Figure 9. The contour colors represent the relative displacement amplitude of the deformed mode shape obtained from the modal analysis. The modal shapes are displayed in scaled form for visualization purposes; therefore, the contour distribution should be interpreted as a relative representation of the deformation pattern rather than as an indication of actual displacement demand under earthquake loading. Mode 1 is translation in the x direction, mode 2 is translation in the y direction and 3rd mode is torsion. In addition, the highest effective MPR (58.0 %) in the x direction was obtained in the 1st mode. In the y direction, the highest effective MPR (69.3 %) was obtained in the 2nd mode, in the z direction, the highest effective MPR (10.94 %) was obtained in the 3rd mode.



Mode 1 / *f1*: 11.17 Hz	Mode 2/ *f2*: 13.14 Hz	Mode 3/ *f3*: 17.75 Hz
MPR x: 58.0 %	MPR y: 69.3 %	MPR y: 10.94 %

Figure 9. 3 Mode shapes and frequencies of the structure (MPR: Mass Participation Ratio)

5.2. Nonlinear Static (Pushover) Analyses

To ascertain the lateral load-bearing capacity of the building, nonlinear static analyses were previously executed in both transversal and longitudinal directions. The foundational principle of this method relies on nonlinear computations designed to assess the seismic response of structures subjected to applied forces. This approach fundamentally involves the application of incremental horizontal forces to the structures, escalating these forces until a predetermined limit value is reached.

This technique produces a base shear force curve relative to displacement at a certain control point on the structure. This curve, known as the capacity curve, helps determine the structure's load-bearing capacity under horizontal loads [65, 66]. For the structures under investigation, nonlinear static analyses were conducted to generate curves illustrating the development of the base shear force-to-building weight ratio (V_t/W) relative to the top displacement. The nonlinear static results (capacity curves) were obtained using control points defined at the upper parts of the building in the transversal and longitudinal directions, as shown in Figure 10. These points were selected to represent the global displacement demand of the structure in the corresponding loading directions and to monitor the regions expected to exhibit the most significant lateral response under seismic action [67]. According to nonlinear static analysis results, the transversal direction resists a maximum of 1.37 g. However, longitudinal direction resists maximum 1.59 g. The maximum crack width observed was 14.03 mm in the transversal direction and 11.74 mm in the longitudinal direction.

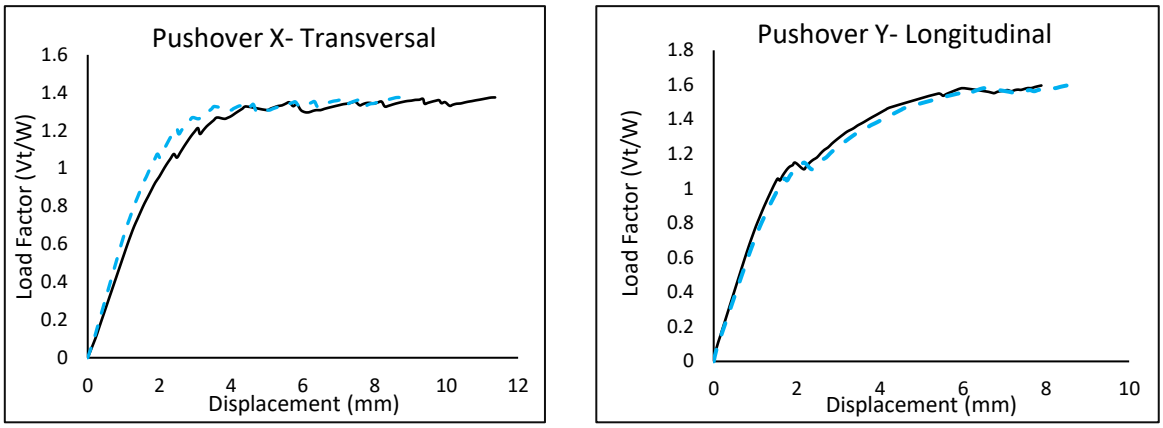


Figure. 10 Capacity curves of the structure

5.3. Nonlinear Time History Analyses

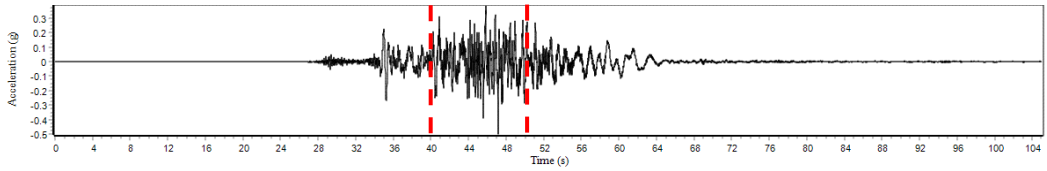
Nonlinear time history analyses (NTHA) have been carried out on the finite element models to examine how the structure behaves during an earthquake. Three different earthquake records (2023 Kahramanmaraş Elbistan, 1999 Kocaeli and 1976 San Fernando) have been selected for the nonlinear analyses. Similar to the recent studies, the analyses employed an effective 10-seconds of the seismic records [48, 68]. The earthquake accelerations applied to the structure in the x direction (transversal direction). Before the NLTHA, a pushover analyses performed in both horizontal directions (x, y). According to the pushover results, the x direction (transversal) was found to be the weak direction of the structure. The vertical component of ground motion was neglected in the nonlinear time-history analyses because the investigated structure is a low-rise masonry building, where structural damage is primarily governed by lateral in-plane and out-of-plane responses. This assumption is consistent with common practices in nonlinear seismic assessment of similar masonry buildings [34, 69]. The earthquake records used in the analysis were taken from the Peer Strong Motion Database NGA-West 2 (PEER) [70] and the Turkish Acceleration Data and Analysis System [6]. Rayleigh damping proportional to mass and stiffness is used in NLTHAs. The damping ratio is considered as 5% as recommended in similar studies [20, 47, 50]. Rayleigh damping coefficients were determined by considering two selected vibration modes of the structure. The coefficients were calculated to achieve a 5% critical damping ratio at the selected modal frequencies, ensuring realistic representation of structural energy dissipation during dynamic analyses. The frequency characteristics of an earthquake have a significant impact on the seismic response of a structure. Important measurements for assessing the frequency characteristics of seismic occurrences include the dominant period, average period, intensity of the power spectrum, and the ratio of peak ground acceleration (PGA) in g units to peak ground velocity (PGV) in meters per second. The inclusion of these criteria is crucial in order to conduct a thorough evaluation of the effect of an earthquake on the structural stability [71, 72]. The PGA/PGV ratio is a straightforward and informative measure for analyzing the frequency characteristics of an earthquake. Earthquake motions are categorized into three groups based on the ratio of peak ground acceleration (PGA) to peak ground velocity (PGV). A ratio larger than 1.2 indicates a high frequency content, a ratio between 0.8 and 1.2 suggests an intermediate frequency content, and a ratio less than 0.8 signifies a low frequency content. This classification system simplifies the interpretation of seismic data by providing a distinct structure to comprehend the frequency characteristics of earthquake movements [73].

The frequency content of earthquakes is evaluated by using the ratio of PGA to PGV. As shown in Table 3. 2023 Kahramanmaraş Elbistan, 1999 Kocaeli and 1976 San Fernando earthquakes are high, low, and intermediate frequency motions, respectively.

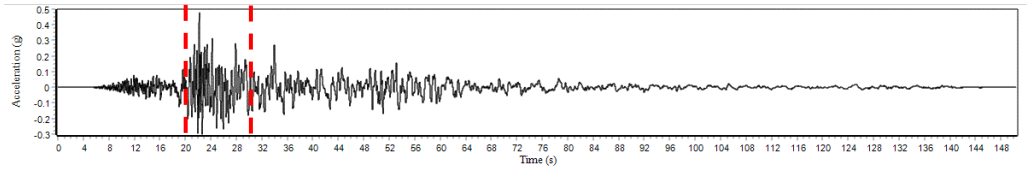
Table 3. Selected earthquake characteristic

No	Earthquake	Record Station/ Horizontal Direction	Magnitude (M_w)	Scale Factor	PGA (g)	PGV (m/s)	PGA/PGV	Distance (km)	V_s (m/s)
1	2023 Kahramanmaraş Elbistan	4406/ E	7.6	1.06	0.47	0.22	2.14	60.7	815
2	1999 Kocaeli	Ambarlı/ ATS000	7.51	1.92	0.25	0.37	0.68	68.1	175
3	1976 San Fernando	Pacoima Dam (upper left abut)/ PUL 164	6.61	0.40	1.21	1.14	0.98	0	2016

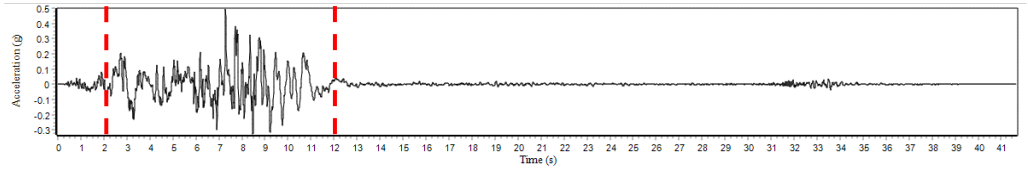
In this paper, near-fault ground motion term refers to the peak ground velocity/peak ground acceleration (PGV/PGA) value greater than 0.1 s [56, 74-77]. Based on the near-fault/far-fault classification criterion adopted in this study, the 1976 San Fernando record was classified as a near-fault ground motion, whereas the 2023 Kahramanmaraş Elbistan and 1999 Kocaeli records were classified as far-fault ground motions. The selection of earthquake records adhered to the guidelines established by the Turkish Building Earthquake Code (TBEC 2018) [41]. Consequently, the earthquake records intended for time history analyses must be scaled in accordance with the horizontal elastic design spectrum. This scaling is based on the geographical coordinates of the structure, the local soil classification, and the designated level of earthquake ground motion. The selected ground motion records were scaled to match the target design spectrum defined according to the seismic hazard level and local soil conditions of the building location. Spectral matching was performed using SeismoMatch software to ensure compatibility between the selected records and the target response spectrum [78]. The compatibility was achieved by minimizing the difference between the mean spectrum of the scaled records and the target spectrum within the period range controlling the structural response. Additionally, Table 4 offers comprehensive details regarding the earthquakes chosen for the analysis. Figure 11 presents the scaled acceleration-time graphs for these selected earthquakes. Figure 12 illustrates both the target elastic design spectrum and the acceleration spectrum of the selected earthquake records.



a) 2023 Kahramanmaraş Elbistan earthquake



b) 1999 Kocaeli earthquake



c) 1976 San Fernando earthquake

Figure 11. Scaled earthquake records

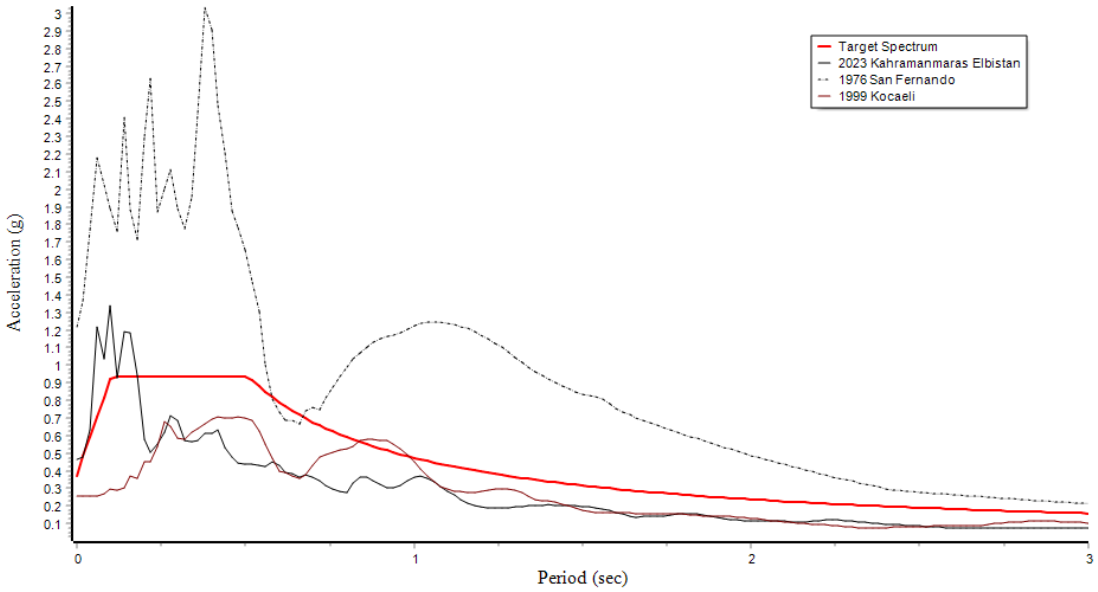


Figure 12. Target spectrum and spectral accelerations

Table 4. Time history analyses results

	2023 Kahramanmaraş Elbistan	1999 Kocaeli	1976 San Fernando	Average of three earthquakes
Normalized displacement (%)	0.18	0.17	0.14	0.16
Max. Crack width (mm)	1.55	0.72	0.45	0.91
Max. inter story Drift ratio (%)	0.31	0.28	0.23	0.27

The tensile strain contour plots and crack widths obtained at the end of the numerical simulations can be shown in Figure 13. It was observed that the crack propagation in the structure after the earthquakes and the crack propagation obtained as a result of numerical analysis are compatible with each other. The seismic response is also evaluated in terms of maximum normalized displacement (displacement divided by height), crack width and maximum interstorey drift ratio. The crack width values obtained at the last step of earthquake records. According to the results, maximum amplitudes were obtained under the 2023 Kahramanmaraş Elbistan earthquake. Hence, tensile strain contours and crack widths were obtained under 2023 Kahramanmaraş Elbistan earthquake.

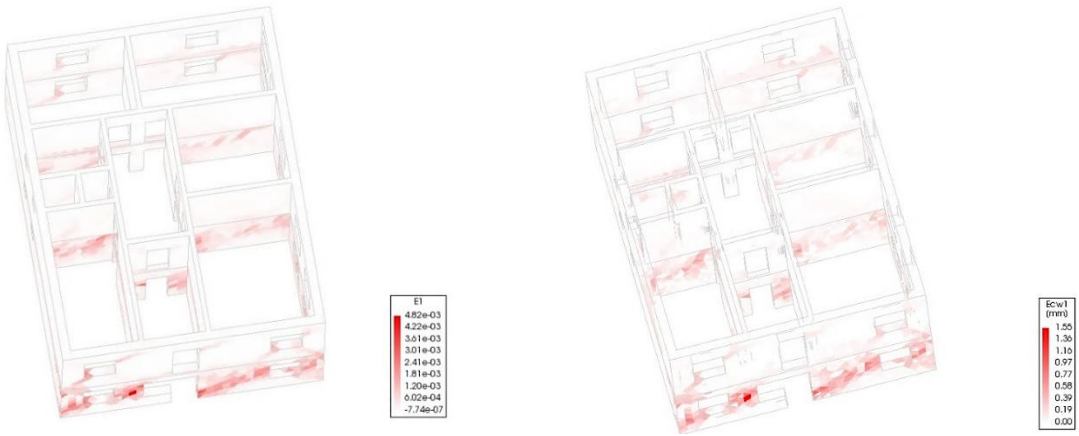


Figure 13. Crack propagation (left) and crack width (right) under the last step of 2023 Kahramanmaraş earthquake

Performance targets expected can be provided with the pushover analyses of the building. It is stated that the performance targets including that the storey drifts with the "Limited Damage", "Controlled Damage", and "Pre-collapse" up to 0.3%,0.7%, and 1% of the building height, respectively, have been attained [79]. According to the Turkish Building Earthquake Code (TBEC) [41], residential buildings should be ensuring "Controlled Damage" performance level. According to the results, under 2023 Kahramanmaraş Elbistan earthquake, limit story drift ratio for the limited damage was exceeded. No global collapse of the structure was observed in the nonlinear analyses; however, the results indicated significant damage concentration and response demand in the critical wall regions.

6. RETROFITTING APPROACH

There are different types of retrofitting methods for improving the seismic resistance of masonry walls in literature. FRP fabrics, stainless strips, steel bars, textile reinforced mortar, steel grid system etc. In this paper, a masonry retrofitting method proposed by Jin et al. [24] was considered. They investigated stainless steel strips reinforcement method binding stainless steel strips to unreinforced masonry walls can significantly enhance both the deformation capacity and load-bearing capacity of the masonry wall. This method effectively integrates the strength of stainless steel with the structural properties of masonry, providing increased resistance to mechanical stresses. The visual representation of the retrofitting process was given in Figure 14. The proposed strengthening method provides a practical solution for improving seismic safety of similar masonry buildings. However, construction feasibility, workmanship quality, and economic considerations may influence field implementation and should be evaluated in future applications.



Figure 14. Visual representation of retrofitting technique adopted from Jin et al. [24]

6.1. Validation of numerical retrofitting model

The retrofitting technique given detailed information above was used to improve the seismic resistance of the case study structure. For this reason, numerical model of the retrofitting method should be validated with experimental study. The experimental results of Jin et al. [24] were used for the validation of the numerical model. The experimental system was modelled with the 3D Finite element method (FEM). Macro modelling technique was considered in the 3D FEM. In the finite element model of the wall, DIANA FEA software was used. Total strain base crack model was selected for nonlinear material behavior of the wall. Detailed information about the total strain base crack model can be found in Section 3. Linear material properties of the wall were taken from Jin et al. [24]. Nonlinear material properties were calculated according to the procedure in Section 3. The nonlinear material properties of the wall are presented in Table 5.

Table 5. Homogenized material properties of validation FEM

Property	Wall	Steel strips
E (MPa)	1500	200000
***Fc* (MPa)**	1.5	-
***Ft* (MPa)**	0.15	565
$\gamma_{masonry}$ **(g/cm^3)**	2.0	7.85
v	0.25	0.30
Gc	2.40	-
Gf	0.0107	-

First, the unreinforced specimen (MW1) was modelled, and analyses conducted. After, reinforced specimen (RMW1) modelled, and analyses conducted. The experimental and numerical results were compared. Wall size is given as 1350 mm × 1350 mm × 240 mm. 3D model and experimental system were shown in Figure 15. Additionally, finite element model of MW1 and RMW1 were given in Figure 16.



Figure 15. 3D model and experimental system [24]

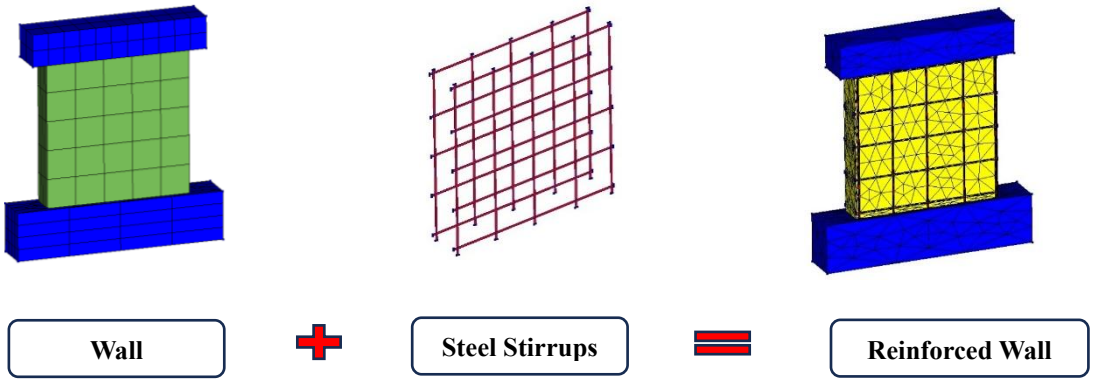


Figure 16. Finite element models of experimental system

Peak displacement and peak force of the experimental wall and numerical results were presented in Table 6. Also, displacement- load curves for the MW1 and RMW1 were given in Figure 17. According to the results, the difference between MW1 and the numerical results is 23.1% and 17.1% for displacement and force, respectively. Additionally, the difference between RMW1 and the reinforced numerical results is 7% and 3% for displacement and force, respectively.

Table 6. Comparison of experimental and numerical results

MW1 (Unreinforced wall)			
	Experimental	Numerical	Difference
Peak displacement (mm)	14	10.76	23.1 %
Peak Force (kN)	75.31	62.41	17.1 %
RMW1 (Reinforced wall)			
	Experimental	Numerical	Difference
Peak displacement (mm)	38.85	41.6	7 %
Peak Force (kN)	87.54	84.8	3 %

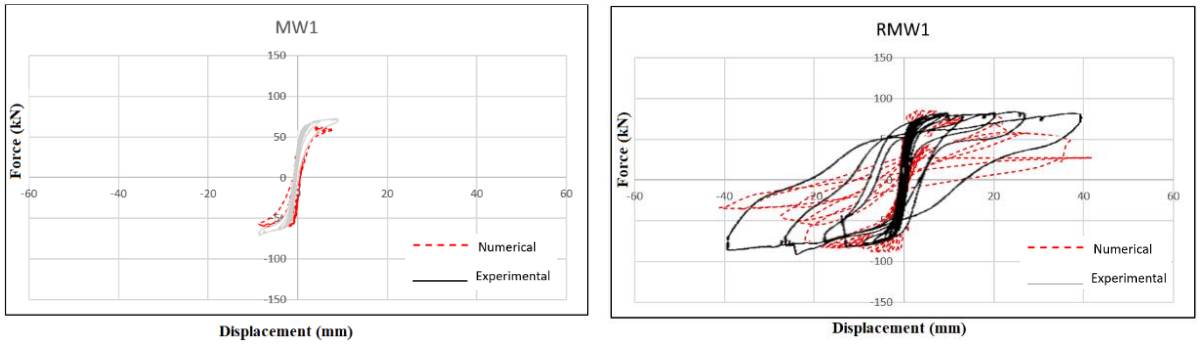


Figure 17. Force- displacement curves for unreinforced and reinforced walls

7. RESULTS FOR THE RETROFITTED STRUCTURE

According to the nonlinear time history analyses results obtained in Section 5, locations of crack propagation were given in Figure 18a. It is seen that tensile damage occurred in the walls marked in Figure 18a. For this reason, the retrofitting method described in detail in section 6 was applied to these walls. The 3D FEM of the retrofitted model can be seen in Figure 18b. The 3D FEM of retrofitted structure consists of 97806 elements, 20938 nodes.

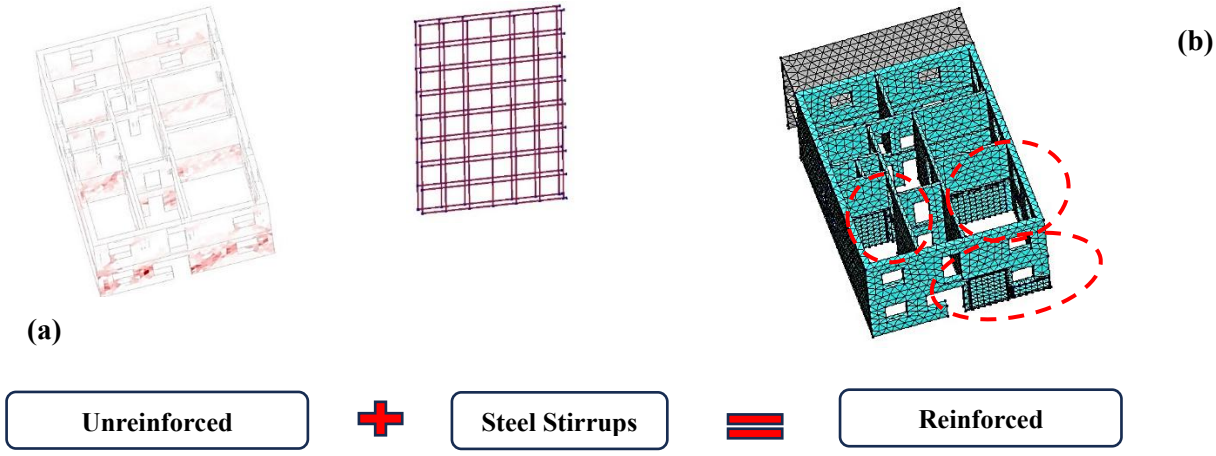


Figure 18. Strengthening scheme and FEM of reinforced structure

In the reinforced structure model, pushover and non-linear time history analyses were performed. Capacity curves of current structure and reinforced structure were given in Figure 19. The load capacity in the transversal direction increased from 1.37g to 2.14g and in the longitudinal direction increased from 1.59g to 2.05g. Also, displacement capacities in each direction were increased.

For the unreinforced structure, the maximum normalized displacement, maximum crack width, and maximum inter-story drift ratio were obtained under the 2023 Kahramanmaraş -Elbistan earthquake. Thus, for the reinforced structure, the 2023 Kahramanmaraş -Elbistan earthquake records were used in the nonlinear time history analyses. A 10-second effective duration of the earthquake records was applied to the structure in the transverse direction. The maximum normalized displacement, maximum crack width, and maximum inter-story drift ratio were obtained through time history analysis and compared with the results of the time history analysis of the unreinforced structure. Comparation of the nonlinear time history analyses results presented in Table 7. In addition, the distribution of tensile strain and crack width at the end of the time history analysis under the 2023 Kahramanmaraş -Elbistan earthquake can be seen in Figure 20. The distribution of tensile strain and crack width of the unreinforced structure is also shown in Figure 20.

Figure 20 clearly demonstrates the effect of the adopted retrofitting intervention on the crack-width distribution of the masonry building. In the unretrofitted model, crack concentrations are mainly observed at the lower wall regions, around openings, and along several wall panels, indicating

significant local damage accumulation under the selected earthquake record. In contrast, the retrofitted model exhibits a substantially reduced crack-width distribution, both in terms of intensity and spatial extent. This result indicates that the applied strengthening scheme effectively reduced local damage concentration and improved the overall seismic response of the structure.

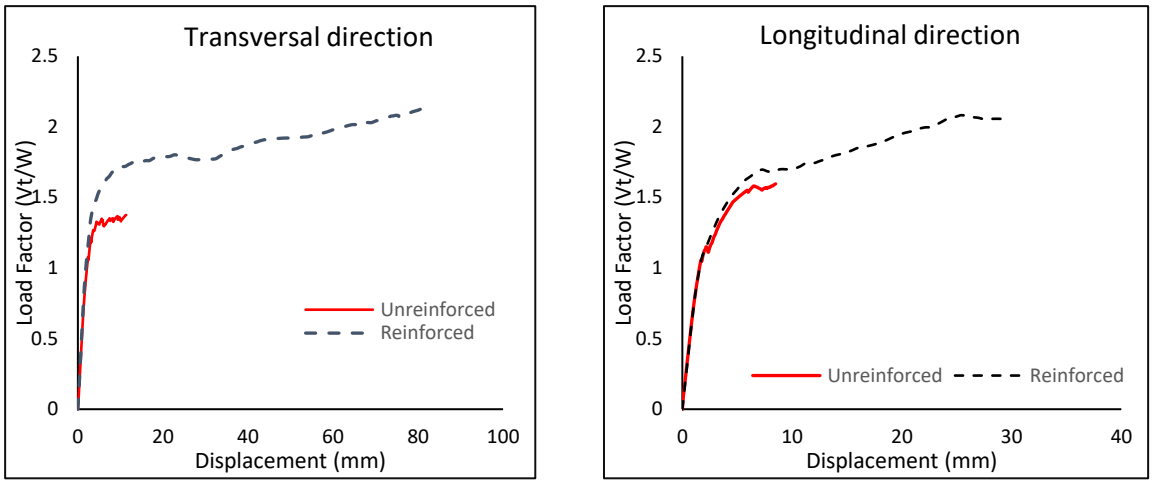


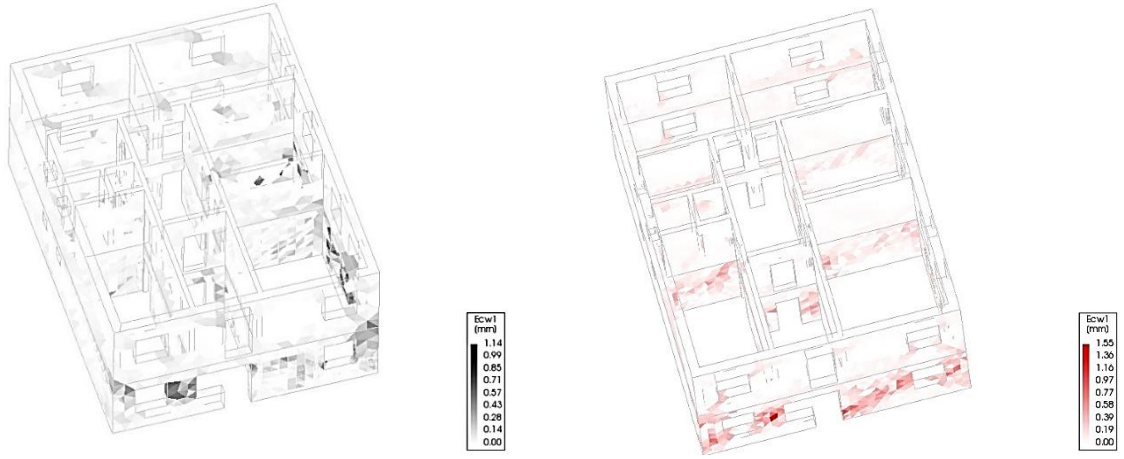
Figure 19. Comparison of capacity curves

Table 7. Comparation of the nonlinear time history analyses results

	2023 Kahramanmaraş Elbistan earthquake		
	Unreinforced	Reinforced	Difference (%)
Normalized displacement (%)	0.18	0.12	-33.3
Max. Crack width (mm)	1.55	1.14	-26.5
Max. inter story Drift ratio (%)	0.31	0.14	-54.8

According to the results of the nonlinear time history analyses, the maximum normalized displacement, maximum crack width, and maximum inter-story drift ratio values decreased in the strengthened structure. While the structure in its current condition does not meet the limited damage performance target according to TBEC [41], it deviates from this target after being retrofitted.

While selected retrofitting method, have not changed the dynamic response of the structure, it decreased the amplitudes related the seismic vulnerability of the structure. In addition, this method has not increased the mass of structure. Therefore, this method is easily applicable and effective in improving seismic resistance of the structure.



a) Retrofitted model b) Unretrofitted model

Figure 20. Distribution of tensile strain and crack width

8. CONCLUSIONS

This study investigated a masonry building in Malatya that survived the 6 February 2023 Kahramanmaraş earthquake sequence. The assessment included a visual damage survey and nonlinear finite element analyses representing both as-built and retrofitted conditions. Nonlinear pushover and time-history analyses were performed to identify critical damage zones and evaluate seismic performance. The retrofit configuration adopted from the literature was numerically validated and then applied to the investigated building.

According to the analyses results:

- The as-built model did not satisfy the LS performance level under the selected Elbistan ground-motion records. After retrofitting, the structure satisfied the LS performance level under the same earthquake records.
- The applied retrofit consists of steel stirrups, and it enhanced the building's seismic resistance by increasing the base shear capacity (from 1.37g to 2.14g and from 1.59g to 2.05g in the two principal directions) while reducing deformation demands in the nonlinear analyses.
- The maximum normalized displacement, maximum crack width, and maximum inter-story drift ratio were obtained through time history analysis and compared with the results of the time history analysis of the unreinforced structure. According to the results of the nonlinear time history analyses, the maximum normalized displacement, maximum crack width, and maximum inter-story drift ratio values decreased as 33.3%, 26.5% and 54.8%, respectively in the strengthened numerical model.
- Türkiye is located in a region that is constantly threatened by earthquakes. Hence, seismic performance of structures should be investigated. Especially, there are a lot of masonry houses in the rural areas of Türkiye and most of these masonry houses have not received engineering services. Therefore, investigation of seismic performance of masonry houses is an important task. In addition, if the level of performance required by the local seismic code has not been met, a retrofitting method should be considered, and numerical FE analysis of the retrofit case should be performed.

Conflict of Interest Statement

There is no conflict of interest between the authors.

Statement of Research and Publication Ethics

The study is complied with research and publication ethics.

Artificial Intelligence (AI) Contribution Statement

The authors used AI-assisted tools only for limited language editing. All scientific interpretation, methodology, analysis, and final manuscript preparation were performed and verified by the authors.

Contributions of the Authors

Alper ÖZMEN: Post-earthquake damage survey; Numerical Analysis, Modelling, Data Gathering, Writing—review & editing; Writing—original draft. Talha SARICI: Soil Survey; Post-earthquake damage survey; Data Gathering, Methodology; Writing—original draft; Writing—review & editing. All authors agree to publish this version of the manuscript.

REFERENCES

[1] J. Ortega, G. Vasconcelos, H. Rodrigues, M. Correia, and P. B. Lourenço, "Traditional earthquake resistant techniques for vernacular architecture and local seismic cultures: A literature review," *J. Cult. Herit.*, vol. 27, pp. 181–196, 2017.

[2] M. ElGawady, P. Lestuzzi, and M. Badoux, "A review of conventional seismic retrofitting techniques for URM," in *Proc. 13th Int. Brick Block Masonry Conf.*, vol. 4, 2004.

[3] S. Bhattacharya, S. Nayak, and S. C. Dutta, "A critical review of retrofitting methods for unreinforced masonry structures," *Int. J. Disaster Risk Reduct.*, vol. 7, pp. 51–67, 2014.

[4] F. Yavartanoo and T. H. K. Kang, "Retrofitting of unreinforced masonry structures and considerations for heritage-sensitive constructions," *J. Build. Eng.*, vol. 49, Art. no. 103993, 2022.

[5] A. Flora et al., "Liquefaction effects in the city of Gölbaşı: From the analysis of predisposing factors to damage survey," *Eng. Geol.*, vol. 338, Art. no. 107633, 2024.

[6] AFAD, *Afet ve Acil Durum Yönetimi Başkanlığı*. Ankara, Türkiye, 2020.

[7] O. Uzdil, T. Coşgun, B. Sayin, and C. Akcay, "Seismic performance evaluation and strengthening proposal for a reconstruction project of a historic masonry building demolished in the 1940s," *J. Build. Eng.*, vol. 66, Art. no. 105914, 2023.

[8] N. Damiani, M. Miglietta, G. Guerrini, and F. Graziotti, "Numerical assessment of the seismic performance of a timber retrofit solution for unreinforced masonry buildings," *Int. J. Archit. Herit.*, vol. 17, no. 1, pp. 114–133, 2023.

[9] F. Ranjbaran and M. Kianibakhsh, "Seismic performance assessment of confined masonry buildings based on displacement," *AUT J. Civ. Eng.*, vol. 5, no. 2, pp. 225–244, 2021.

[10] T. Coşgun, O. Uzdil, B. Sayin, and K. K. Zengin, "Seismic vulnerability assessment of a masonry structure and an FRP-strengthening proposal," *Case Stud. Constr. Mater.*, vol. 17, Art. no. e01680, 2022.

[11] H. Bilgin, N. Shkodrani, M. Hysenlliu, H. B. Özmen, E. Isik, and E. Harirchian, "Damage and performance evaluation of masonry buildings constructed in 1970s during the 2019 Albania earthquakes," *Eng. Fail. Anal.*, vol. 131, Art. no. 105824, 2022.

[12] A. I. Çarhoğlu and K. A. Korkmaz, "Evaluation of earthquake behavior of an existing masonry building," *J. Adv. Technol. Sci.*, vol. 2, no. 1, pp. 1–11, 2013.

[13] A. Özmen, Ö. F. Taş, O. İnce, M. Atar, and E. Sayın, "2023 Kahramanmaraş depremleri sonrası Malatya ilinde yer alan yığma binaların hasar mekanizmasının incelenmesi," (in Turkish), *Niğde Ömer Halisdemir Üniv. Mühendislik Bilimleri Derg.*, vol. 13, no. 2, pp. 697–703, 2024.

[14] İ. Ö. Dedeoğlu, M. Yetkin, H. Erkek, and Y. Calayır, "Nonlinear earthquake response of the historic Ahi Musa Masjid," in *Proc. 3rd Int. Civ. Eng. Archit. Congr. (ICEARC'23)*, 2023.

[15] İ. Kocaman and İ. Gürbüz, "Enhancing seismic performance of historic mosques through retrofitting measures," *Eng. Struct.*, vol. 301, Art. no. 117245, 2024.

[16] A. E. Akan et al., "Seismic evaluation of a renovated wooden hypostyle structure: A case study on a mosque designed with the combination of Asian and Byzantine styles in the Seljuk Era (14th Century AD)," *J. Build. Eng.*, vol. 43, Art. no. 103112, 2021.

[17] M. Betti and L. Galano, "Seismic analysis of historic masonry buildings: The Vicarious Palace in Pescia (Italy)," *Buildings*, vol. 2, no. 2, pp. 63–82, 2012.

[18] B. Yildizlar, "Seismic performance analysis and rehabilitation applications for a historical masonry building through field works and experimental investigations," *Struct.*, vol. 34, pp. 1811–1833, 2021.

[19] B. Güneş, A. Mangır, and V. Okumuş, "Assessment of an existing masonry structure using linear and nonlinear material models," in *Proc. 4th Conf. Smart Monitoring Assess. Rehabil. Civ. Struct.*, 2017.

[20] İ. Kocaman and İ. Kazaz, "Collapse mechanism of historical masonry mosques under strong ground motions," *Eng. Fail. Anal.*, vol. 144, Art. no. 106983, 2023.

[21] A. Aşıkoğlu, Ö. Avşar, P. B. Lourenço, and L. C. Silva, "Effectiveness of seismic retrofitting of a historical masonry structure: Kütahya Kurşunlu Mosque, Turkey," *Bull. Earthq. Eng.*, vol. 17, no. 6, pp. 3365–3395, 2019.

[22] M. M. Maraş, A. Özmen, E. Sayın, and Y. Ayaz, "Seismic assessment of the historical Sütlü Minaret Mosque," *Period. Polytech. Civ. Eng.*, vol. 66, no. 2, pp. 445–449, 2022, doi: 10.3311/PPci.18195.

[23] M. Zizi, F. Campitiello, and G. De Matteis, "A retrofitting technique using steel grids for existing masonry panels: A numerical and analytical study," *Bull. Earthq. Eng.*, vol. 19, no. 2, pp. 1051–1077, 2021.

[24] Y. H. Jin, Z. Y. Zhou, B. L. Bao, H. Y. Wang, and T. Wang, "Experimental study on the seismic performance of clay brick masonry wall strengthened with stainless steel strips," *J. Build. Eng.*, vol. 69, Art. no. 106076, 2023.

[25] G. Rinaldin, C. Miniussi, and C. Amadio, "Cyclic behavior of masonry walls strengthened by tie rods," *Eng. Struct.*, vol. 184, pp. 287–300, 2019.

[26] P. Aghabeigi and S. Farahmand-Tabar, "Seismic vulnerability assessment and retrofitting of historic masonry building of Malek Timche in Tabriz Grand Bazaar," *Eng. Struct.*, vol. 240, Art. no. 112418, 2021.

[27] S. Tanriverdi, "An experimental and numerical study of the strengthening of masonry brick vaults," *Struct.*, vol. 47, pp. 800–813, 2023.

[28] A. Gattulli, G. Lampis, G. Marcari, and A. Paolone, "Simulations of FRP reinforcement in masonry panels and application to a historic facade," *Eng. Struct.*, vol. 75, pp. 604–618, 2014.

[29] M. U. Saleem, M. Numada, M. N. Amin, and K. Meguro, "Shake table tests on FRP retrofitted masonry building models," *J. Compos. Constr.*, vol. 20, no. 5, Art. no. 04016031, 2016.

[30] L. A. S. Kouris and T. C. Triantafillou, "State-of-the-art on strengthening of masonry structures with textile reinforced mortar (TRM)," *Constr. Build. Mater.*, vol. 188, pp. 1221–1233, 2018.

[31] C. Caggegi, E. Lanoye, K. Djama, A. Bassil, and A. Gabor, "Tensile behaviour of a basalt TRM strengthening system: Influence of mortar and reinforcing textile ratios," *Compos. Part B Eng.*, vol. 130, pp. 90–102, 2017.

[32] B. Torres, S. Ivorra, F. J. Baeza, L. Estevan, and B. Varona, "Textile reinforced mortars (TRM) for repairing and retrofitting masonry walls subjected to in-plane cyclic loads: An experimental approach," *Eng. Struct.*, vol. 231, Art. no. 111742, 2021.

[33] C. G. Papanicolaou, T. C. Triantafillou, K. Karlos, and M. Papathanasiou, "Textile-reinforced mortar (TRM) versus FRP as strengthening material of URM walls: In-plane cyclic loading," *Mater. Struct.*, vol. 40, pp. 1081–1097, 2007.

[34] G. Camata, A. Di Primio, V. Sepe, and C. Cantagallo, "The effect of the vertical component of the earthquake on a regular masonry wall," *Appl. Sci.*, vol. 13, no. 4, Art. no. 2459, 2023.

[35] E. Işık et al., "Structural damages in masonry buildings in Adıyaman during the Kahramanmaraş (Türkiye) earthquakes (Mw 7.7 and Mw 7.6) on 06 February 2023," *Eng. Fail. Anal.*, vol. 151, Art. no. 107405, 2023.

[36] E. Işık et al., "Seismic performances of masonry educational buildings during the 2023 Türkiye (Kahramanmaraş) earthquakes," *GeoHazards*, vol. 5, no. 3, pp. 700–731, 2024.

[37] R. İzol, E. Işık, F. Avcil, M. H. Arslan, E. Arkan, and A. Büyüksaraç, "Seismic performance of masonry structures after 06 February 2023 earthquakes: Site survey and FE modelling approach," *Soil Dyn. Earthq. Eng.*, vol. 186, Art. no. 108904, 2024.

[38] R. T. Özcan, "Malatya ili için sıvılaşma, taşıma gücü ve diğer geoteknik özelliklerin coğrafi bilgi sistemi kullanılarak değerlendirilmesi," M.S. thesis, Department of Civil Engineeering, İnönü Univ., Malatya, Türkiye, 2023.

[39] T. Sarici and R. T. Ozcan, "Evaluation of geotechnical properties of Doğanşehir district with geographical information systems after the February 6, 2023 earthquakes," *J. Seismol.*, vol. 28, pp. 1421–1444, 2024.

[40] H. B. Seed and I. M. Idriss, "Simplified procedure for evaluating soil liquefaction potential," *J. Soil Mech. Found. Div.*, vol. 97, no. 9, pp. 1249–1273, 1971.

[41] TBEC, *Turkish Building Earthquake Code 2018*. Ankara, Türkiye: Disaster and Emergency Management Agency (AFAD), 2018.

[42] A. S. Vesic, "Bearing capacity of shallow foundations," in *Foundation Engineering Handbook*. New York, NY, USA: Reinhold, 1975.

[43] K. Terzaghi, *Theoretical Soil Mechanics*. New York, NY, USA: Wiley, 1943.

[44] Turgutlu Yüksel Tuğla Kiremit, *Brick Feature Catalogue*. Manisa, Türkiye, 2023.

[45] P. Lourenco, "Computational strategy for masonry structures," Ph.D. dissertation, Delft Univ. Technol., Delft, The Netherlands, 1996.

[46] A. Carpinteri, S. Invernizzi, and G. Lacidogna, "In situ damage assessment and nonlinear modelling of a historical masonry tower," *Eng. Struct.*, vol. 27, no. 3, pp. 387–395, 2005.

[47] A. Özmen and E. Sayın, "3D soil structure interaction effects on the seismic behavior of single span historical masonry bridge," *Geotech. Geol. Eng.*, vol. 41, no. 3, pp. 1637–1653, 2023.

[48] E. Hökelekli and A. Al-Helwani, "Effect of soil properties on the seismic damage assessment of historical masonry minaret–soil interaction systems," *Struct. Des. Tall Spec. Build.*, vol. 29, no. 2, Art. no. e1694, 2020.

[49] O. Onat, F. Deniz, A. Özmen, E. Özdemir, and E. Sayın, "Performance evaluation and damage assessment of historical Yusuf Ziya Pasha Mosque after February 6, 2023 Kahramanmaraş earthquakes," *Struct.*, vol. 58, Art. no. 105415, 2023.

[50] İ. Kocaman and İ. Kazaz, "Global drift ratio limits for historical masonry mosques," *Bull. Earthq. Eng.*, vol. 21, no. 5, pp. 3011–3040, 2023.

[51] H. Bilgin and O. Korini, "Seismic capacity evaluation of unreinforced masonry residential buildings in Albania," *Nat. Hazards Earth Syst. Sci.*, vol. 12, no. 12, pp. 3753–3764, 2012.

[52] S. Gönen and S. Soyöz, "Seismic analysis of a masonry arch bridge using multiple methodologies," *Eng. Struct.*, vol. 226, Art. no. 111354, 2021.

[53] D. Proske and P. Van Gelder, *Safety of Historical Stone Arch Bridges*. Berlin, Germany: Springer, 2009.

[54] *Guideline for Load and Resistance Assessment of Existing European Railway Bridges: Advices on the Use of Advanced Methods*, RIL 805, COWI A/S, 2007.

[55] A. Baykasoğlu, H. Güllü, H. Çanakçı, and L. Özbakır, "Prediction of compressive and tensile strength of limestone via genetic programming," *Expert Syst. Appl.*, vol. 35, no. 1–2, pp. 111–123, 2008.

[56] A. Bayraktar and E. Hökelekli, "Nonlinear soil deformability effects on the seismic damage mechanisms of brick and stone masonry arch bridges," *Int. J. Damage Mech.*, vol. 30, no. 3, pp. 431–452, 2021.

[57] M. Karaton, H. S. Aksoy, E. Sayın, and Y. Calayır, "Nonlinear seismic performance of a 12th century historical masonry bridge under different earthquake levels," *Eng. Fail. Anal.*, vol. 79, pp. 408–421, 2017.

[58] H. Y. Ersoy, *Composite Material*. Istanbul, Türkiye: Literature, 2001.

[59] *Design of Masonry Structures—Part 1-1: General Rules for Reinforced and Unreinforced Masonry Structures*, Eurocode 6. Brussels, Belgium: Comité Européen de Normalisation, 2005.

[60] A. Özmen, "Seismic performances of different strengthening techniques in masonry residential buildings," *Teh. Vjesn.*, vol. 33, no. 2, pp. 470–486, 2026.

[61] DIANA FEA, *User's Manual Release 10.5*. The Netherlands, 2022.

[62] P. B. Lourenço and J. M. Pereira, *Seismic Retrofitting Project: Recommendations for Advanced Modelling of Historic Earthen Sites*. Los Angeles, CA, USA: Getty Conservation Institute, 2018.

[63] T. Krejčí, T. Koudelka, V. Bernardo, and M. Šejnoha, "Effective elastic and fracture properties of regular and irregular masonry from nonlinear homogenization," *Comput. Struct.*, vol. 254, Art. no. 106580, 2021.

[64] M. Valente and G. Milani, "Seismic response and damage patterns of masonry churches: Seven case studies in Ferrara, Italy," *Eng. Struct.*, vol. 177, pp. 809–835, 2018.

[65] A. K. Chopra and R. K. Goel, "A modal pushover analysis procedure for estimating seismic demands for buildings," *Earthq. Eng. Struct. Dyn.*, vol. 31, no. 3, pp. 561–582, 2002.

[66] F. Minghini, E. Bertolesi, A. del Grosso, G. Milani, and A. Tralli, "Modal pushover and response history analyses of a masonry chimney before and after shortening," *Eng. Struct.*, vol. 110, pp. 307–316, 2016.

[67] S. Tiberti, M. Acito, and G. Milani, "Comprehensive FE numerical insight into Finale Emilia Castle behavior under 2012 Emilia Romagna seismic sequence: Damage causes and seismic vulnerability mitigation hypothesis," *Eng. Struct.*, vol. 117, pp. 397–421, 2016.

[68] M. Valente, G. Barbieri, and L. Biolzi, "Seismic assessment of two masonry Baroque churches damaged by the 2012 Emilia earthquake," *Eng. Fail. Anal.*, vol. 79, pp. 773–802, 2017.

[69] I. Tomić, A. Penna, I. Senaldi, G. Magenes, and V. Kilar, "Numerical simulation of unreinforced masonry buildings with timber diaphragms," *Buildings*, vol. 11, no. 5, Art. no. 205, 2021.

[70] PEER, "NGA West 2," *Pacific Earthquake Engineering Research Center*. Accessed: Jan. 12, 2025. [Online]. Available: https://peer.berkeley.edu/research/nga-west-2

[71] E. M. Rathje, F. Faraj, S. Russell, and J. D. Bray, "Empirical relationships for frequency content parameters of earthquake ground motions," *Earthq. Spectra*, vol. 20, no. 1, pp. 119–144, 2004.

[72] R. K. McGuire, "Seismic ground motion parameter relations," *J. Geotech. Eng. Div.*, vol. 104, no. 4, pp. 481–489, 1978.

[73] W. K. Tso, T. J. Zhu, and A. C. Heidebrecht, "Engineering implication of ground motion A/V ratio," *Soil Dyn. Earthq. Eng.*, vol. 11, no. 3, pp. 133–144, 1992.

[74] W. I. Liao, C. H. Loh, and B. H. Lee, "Comparison of dynamic response of isolated and non-isolated continuous girder bridges subjected to near-fault ground motions," *Eng. Struct.*, vol. 26, no. 14, pp. 2173–2183, 2004.

[75] S. Zhang and G. Wang, "Effects of near-fault and far-fault ground motions on nonlinear dynamic response and seismic damage of concrete gravity dams," *Soil Dyn. Earthq. Eng.*, vol. 53, pp. 217–229, 2013.

[76] A. K. Chopra and C. Chintanapakdee, "Comparing response of SDF systems to near-fault and far-fault earthquake motions in the context of spectral regions," *Earthq. Eng. Struct. Dyn.*, vol. 30, no. 12, pp. 1769–1789, 2001.

[77] K. Galal and A. Ghobarah, "Effect of near-fault earthquakes on North American nuclear design spectra," *Nucl. Eng. Des.*, vol. 236, no. 18, pp. 1928–1936, 2006, doi: 10.1016/j.nucengdes.2006.02.019.

[78] Seismosoft Ltd., *Seismomatch: Earthquake Software for Response Spectrum Matching*, 2021.

[79] General Directorate of Foundations, *Seismic Risks Management Guide for Historical Structures (SRMGHS)*. Ankara, Türkiye, 2017.